

Why to Use Self Assembled Metallic Nanoparticles Template for Metal Electrodeposition: Metallic Nanostructures with Controlled Morphologies and Adjustable Wetting Properties

A. Taleb*, X. Yanpeng

UPMC –LECIME/ENSCP/Chimie paristech/CNRS7575, 11, Rue P. & M. Curie, 75231 Paris, France

(Received 14 June 2013; published online 31 August 2013)

We investigated the benefits of using self assembled gold nanoparticles (Au NPs) template for metal electrodepositions. For short electrodeposition time, surface patterning was achieved and a well dense organized structure with nanometre resolution of metallic nanoparticles was prepared. For longer electrodeposition time, different morphologies were obtained. The mechanisms behind the formation of this morphology were analysed and discussed based on the influence of self-assembled Au NPs template in terms of thiol molecules diffusion and adsorption on metallic deposits. Furthermore adjustable wetting properties were obtained through the tuning of electrodeposition time.

Keywords: Au nanoparticles, Self-assembly, Metal electrodeposition.

PACS numbers: 81.15.Pq, 81.07. – b

1. INTRODUCTION

For different nanotechnological applications the fabrication of nanostructured materials with a well defined pattern size and shape is a key point [1-4]. In fact, the physical properties associated with such material depend on the size [5], the morphology and the organization of the pattern [1]. For the preparation of such nanostructures two approaches were used: direct deposition [6] and deposition on modified substrate [7]. Direct deposition approaches, usually achieve disordered surface structures because of the preferential nucleation at crystalline defects and step edges [8-10]. To overcome this problem a modified substrate with patterns acting as preferential nucleation sites is proposed. However, one of the emerging and promising strategies to create surface patterning and preferential nucleation sites for electrodeposition at a very low scale consists of using a mask made of self-assembled molecular film [11-12] or colloidal particles [13-15]. Furthermore, a few works deal with the use of the particles as a nucleation sites [16-17].

In this works, we illustrate the ability of self assembled Au NPs template to electrocatalyze HOPG surface and to direct electrodeposition of different metals such as Cu and Ag at nanometer scale. This nanostructuring method provides a promising way to control the electrodeposits growth into ordered structure at nanometer resolution. Additionally, we demonstrate that the morphology of metallic electrodeposits can be controlled and different morphologies were obtained. Interestingly, these surface morphologies demonstrate adjustable wetting properties.

2. EXPERIMENTAL

A standard three electrode electrochemical configuration was used to achieve Cu and Ag electrodeposition. The reference and counter electrodes were respectively Ag/AgCl and a platinum sheet. For Cu electrodeposition experiments a clean (0001) highly oriented pyrolyt-

ic graphite (HOPG) surface, which is produced through a cleaving process, was used as a working electrode. The modified HOPG electrode was prepared by depositing a droplet of Au NP solution on the HOPG surface. The area in contact with the solution was fixed at 9 mm². Cu and Ag were deposited respectively from the aqueous solutions of 10⁻³ M CuSO₄ and 1 M H₂SO₄ as the supporting electrolyte and from the aqueous solutions of 10⁻² M AgNO₃ and 1 M HClO₄ as the supporting electrolyte. This solution was deaerated by purified nitrogen for 2 h before use. Copper sulfate pentahydrate (CuSO₄·5H₂O) and sulphuric acid (H₂SO₄) were obtained from Merck whereas Silver nitrate, perchlorate acid and dodecanethiol were obtained from fluka. All chemicals used were analytical grade and used without further purification. The electrolytes were prepared with water purified by Milli Q system (Millipore, electric resistivity 18.2 MΩ·cm).

The 5 nm Au NPs were synthesized using the well known Stucky approach [32]. After synthesis, Au NPs were coated with n-dodecanethiol and presented in a narrow size distribution (6%). All the experiments of Cu and Ag electrodeposition were performed on Au NPs modified HOPG electrodes. The electrodes were prepared by leaving a dilute droplet of Au NP solution with a concentration of 1.2 × 10⁻⁷ M on the HOPG electrode at ambient temperature.

The chronoamperometry was performed at a fixed potential of -0.58 V and -0.3 V versus Ag/AgCl for respectively Cu and Ag electrodeposition. All the electrochemical measurements were performed with an EG&G Princeton Applied Research potentiostat/galvanostat model 273 A.

The morphologies of the Cu electrodeposits, Ag electrodeposits and Au NPs film were studied using a high-resolution Ultra 55 Zeiss field emission gun scanning electron microscope (FEGSEM).

The chemical compositions of all the samples were determined by X-ray photoelectron spectroscopy (XPS) and for the measurements we used a Kratos Analytical

*abdelhafed.taleb@upmc.fr

Axis Ultra DLD, using an Al K α source monochromatized at 1486.6 eV.

The wetting properties of our prepared surfaces in terms of static contact angle were determined using a Krüss DSA10 contact angle measuring apparatus equipped with a CCD camera. A 3 μ l water droplet purified by Milli Q System (Millipore, electric resistivity 18.2 M Ω -cm) was used for the static contact angle measurements.

3. RESULTS AND DISCUSSION

In Fig. 1a is shown typical FEGSEM images of Ag electrodeposits on Au NPs modified HOPG substrate over different electrodeposition time. It is seen that after electrodeposition over 10 s, a small bright spot appears on the modified HOPG electrode corresponding to the formation of Ag NPs. The hexagonal pattern formed by Au NPs is still preserved (indicated by arrow), and Ag deposit is reproducing this structure (indicated by arrow in figure 1(a) and insert). Similar behavior was observed for Cu electrodeposition in same conditions.

Further confirmation of Ag deposition is provided by XPS experiments (Fig. 1(b)). These results evidenced the fact that self assembled Au NPs allows the surface patterning with nanometer resolution which no other techniques can allow [16-18]. By comparing metal electrodeposition on bare HOPG and Au NPs modified HOPG electrode, different surface textures were observed. On bare HOPG the electrodeposition occurs on step edges and terrace defects according to Volmer Weber island mechanism whereas atomic flat terrace are inhibited sites [16-18]. However, on Au NPs modified HOPG, metal electrodeposition behavior is completely different and metal deposition takes place on the whole electrode surface including the atomic flat terrace [16-18]. These results show clearly that Au NPs deposited on the HOPG electrode activate the inhibited sites of atomic flat terrace. The mechanism behind this activation can be understood by taking into account the strain effects of Au NPs on the electronic properties of HOPG electrode [18-19].

For longer electrodeposition time and low deposition temperature (18°C), the FEGSEM images depicted in Fig. 2 show dendrite particles [20-21]. This kind of growth is mainly diffusion controlled locally and accompanied by preferential growth directions [21-22].

Furthermore in the pure diffusion limited aggregation (DLA), the solid growth occurs as random walkers diffuse of metal ion (Ag⁺ or Cu²⁺ in our case) into contact with the growing aggregate [23-24]. This mechanism explains the random orientation of growing silver dendrites. However, with Cu dendrites oriented and dense superstructures were observed. From the FEGSEM experiments it is evidenced that the self assembled Au NPs pattern plays a crucial role in the formation of the observed Cu dendrites' superstructure [21]. In fact the crack defects of the Au NPs template allow micrometer patterning for Cu electrodeposition. A combination of self assembled Au NPs pattern and the aggregation of Cu electrodeposits has been shown to be behind the observed Cu superstructure formation mechanism.

For high electrodeposition temperature of 62°C, different other morphologies were obtained [21]. The results are depicted in Fig. 2. It can be seen that by increasing the temperature more faceted particles were obtained. Ag deposits form plate particles [25] whereas Cu particles are of polyhedral morphology[21]. These results can be understood in terms of dodecanethiol molecules diffusion from Au NPs into the metal deposits surface in which it is adsorbed. Furthermore, dodecanethiol was found to adsorb strongly on the (111) crystallographic facets. As a consequence the growth of this facet slow down through the formation of a dense layer which slow the metal ion reduction on their surface allowing the growth of crystallographic planes in perpendicular directions. This growth anisotropy results in the formation of different observed faceted morphologies.

The wetting properties of electrodeposited silver dendritic film were characterized by the measurement of water contact angles (CAs) [20]. The results are depicted in Fig. 3 and it should be observed that the CA depends on the electrodeposition time. The observed wetting properties are governed by the continuous increase of dendritic surface roughness during the electrodeposition time and the rate coverage of adsorbed dodecanethiol molecules. Thus by varying the silver electrodeposition time adjustable wetting properties can be obtained and a transition between Wenzel and Cassie Baxter state can be induced.

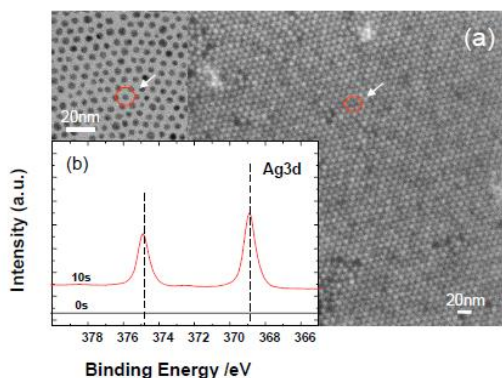


Fig. 1 – (a) FEGSEM images of the electrodeposited silver nanoparticles onto Au NP-modified HOPG electrode at electrodeposition time of 10 s and from an aqueous solution containing 10⁻² M AgNO₃ and 1 M HClO₄ at potential deposition of -0.3 V. Insert is the TEM image of Au NP monolayer (b) XPS core level spectra of Ag 3d acquired from electrodeposited silver on a Au NP modified HOPG electrode over different electrodeposition times 0s and 10 s.

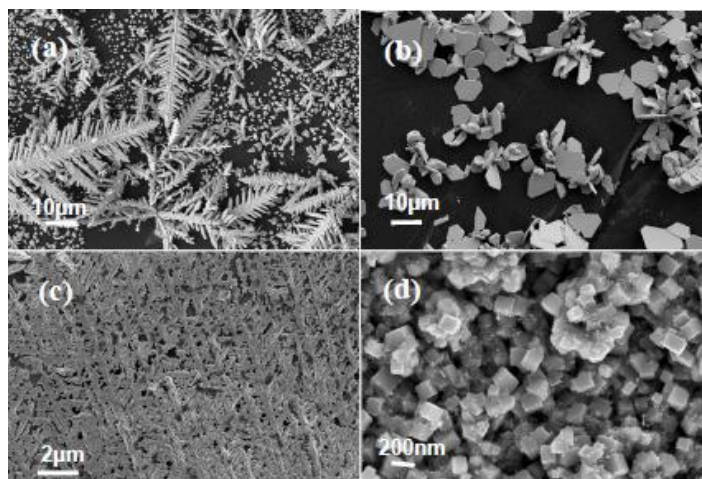


Fig. 2 – FEGSEM images of the electrodeposited silver particles onto Au NP-modified HOPG electrode from an aqueous solution containing 10^{-2} M AgNO_3 and 1 M HClO_4 at potential deposition of -0.3 V and temperature of 18°C (a) and 62°C (b). FEGSEM images of the electrodeposited Copper particles onto Au NP-modified HOPG electrode from an aqueous solution containing 10^{-3} M CuSO_4 and 1 M H_2SO_4 at potential deposition of -0.58 V and temperature of 18°C (c) and 62°C (d).

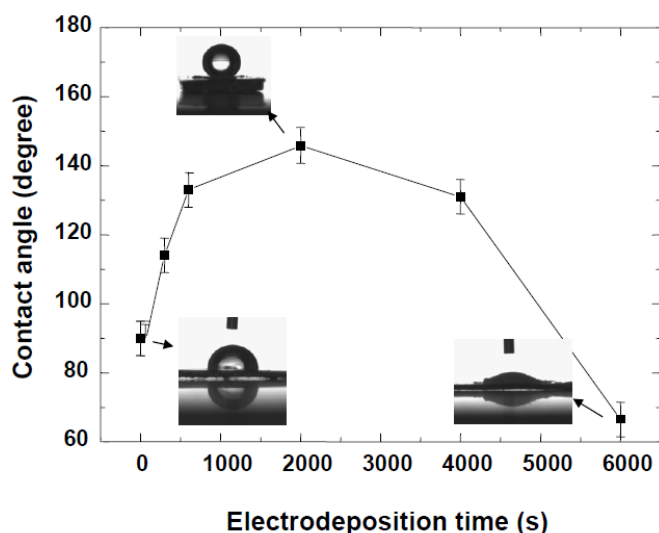


Fig. 3 – Water contact angle measured on the surface of a Au NP-modified HOPG electrode as a function of silver electrodeposition time at $E = -0.3$ V versus Ag/AgCl and from a solution of 10^{-2} M AgNO_3 and 1 M HClO_4 . The insert correspond to the water droplet shape for the indicated conditions

4. CONCLUSIONS

Different advantages of using self assembled Au NPs template for metal electrodeposition were illustrated. It is evidenced that self assembled Au NPs allows the surface patterning with nanometer resolution which no other techniques can achieve. It has been demonstrated that the temperature and applied potential are the key parameters for controlling the morphology of prepared films. Importantly, there exists significant preferential crystal growth during the electrodeposition processes leading to uniform particle morphology. The morphology changes during the electrodeposition process are attributed to thiol molecules' diffusion favored by the increase in the temperature and their preferential adsorption on the (111) crystallographic plane of silver and copper. Furthermore, this work offers new opportunities for functionalized nano-

particles to assist shape selective synthesis of electrodeposited material using modified electrodes by convenient surfactant covered metallic nanoparticles. The present method also offers a new and simple way for large scale synthesis of millimeter scale films. Otherwise, the morphology of the particles in the film should be independent of the conducting substrate nature. By varying the silver electrodeposition time adjustable wetting properties can be obtained

ACKNOWLEDGEMENTS

Authors are grateful to Pierre Dubot at the Institut de chimie et des matériaux Paris Est UMR 7181 for acquiring and discussing the XPS spectra.

REFERENCES

1. R. Walters, J. Biteen, H. Atwater, G. Bourianoff, *Laser Focus World* **40**, 70 (2004)
2. Y. Niquet, G. Allan, C. Delerue, M. Lannoo, *Appl. Phys. Lett.* **77**, 1182 (2000).
3. N.W. Dashiell, U. Denker, C. Muller, G. Costantini, K. Kern, O.G. Schmidt, *Appl. Phys. Lett.* **80**, 1279 (2002).
4. M. Law, L.E. Greene, L.C. Johnson, R. Saykally, P. Yang, *Nature Mater.* **4**, 455 (2005).
5. A. Taleb, C. Petit, M.P. Pileni, *J. Phys. Chem. B*, **102**, 2214 (1998).
6. G.E. Engelmann, J.C. Ziegler, M.D. Kolb, *Surf. Sci.* **401**, L420 (1998).
7. B.C. Bunker, P.C. Rieke, B.J. Tarasevich, A. Campbell, G.E. Fryxell, G.L. Graff, J. Song, J. Liu, J.W. Virden, *Science*, **264**, 48 (1994).
8. R. Ullmann, T. Will, D.M. Kolb, *Chem. Phys. Lett.* **209**, 238 (1993).
9. H. Ling, L. Eun-Sung, K. Kwang-Bum, *Colloids Surf. A* **262**, 125 (2005).
10. H. Liu, F. Favier, K. Ng, M.P. Zach, R.M. Penner, *Electrochim. Acta* **47**, 671 (2001).
11. O. Azzaroni, M.H. Fonticelli, G. Beniter, R.L. Schilardi, R. Gago, I. Caretti, L. Vazquez, R.C. Salvarezza, *Adv. Mater.*, **16**, 405 (2004).
12. M. Zhang, S. Lenhert, M. Wang, L. Chi, N. Lu, H. Fuchs, N. Ming, *Adv. Mater.* **16**, 409 (2004).
13. D. Ito, M.L. Jespersen, J.E. Hutchison, *ACS Nano* **2**, 2001 (2008).
14. J. Huang, A.R. Tao, S. Connor, R. He, P. Yang, *Nano Lett.*, **6**, 524 (2006).
15. C. Li, G. Hong, P. Wang, D. Yu, L. Qi, *Chem. Mater.* **21**, 891 (2009).
16. A. Taleb, C. Mangeney, V. Ivanova, *J. Electrochem. Soc.* **158** No2, K28 (2011).
17. M.G. Montes de Oca, D.J. Fermin, *Electrochim. Acta* **455**, 8986 (2010).
18. A. Taleb, X. Yanpeng, P. Dubot, *J. Electroanal. Chem.* **693** 60 (2013).
19. M. Zhou, A. Zhang, Z. Dai, Y.P. Feng, C. Zhang, *J. Phys. Chem. C* **114**, 16541 (2010).
20. A. Taleb, C. Mangeney, V. Ivanova, *Nanotechnology*, **22**, 205301 (2011).
21. A. Taleb, X. Yanpeng, *Electrochimica Acta* 2013, in press.
22. C. Yan, D. Xue, *Crystal Growth Design* **8**, 1849 (2008)
23. A.A. Aviziens, C.M. Olmos, H.O. Sillin, M. Aono, J.K. Gimzewski, A.Z. Stieg, *Crystal Growth Design* **13**, 465 (2013).
24. M. Matsushita, M. Sano, Y. Hayakawa, H. Honjo, Y. Sawada, *Phys. Rev. Lett.* **53**, 286 (1984).
25. A. Taleb, X. Yanpeng, S. Munteanu, F. Kanoufi, P. Dubot, *Electrochimica Acta* **88**, 621 (2013).